



저작자표시-비영리-변경금지 2.0 대한민국

이용자는 아래의 조건을 따르는 경우에 한하여 자유롭게

- 이 저작물을 복제, 배포, 전송, 전시, 공연 및 방송할 수 있습니다.

다음과 같은 조건을 따라야 합니다:



저작자표시. 귀하는 원저작자를 표시하여야 합니다.



비영리. 귀하는 이 저작물을 영리 목적으로 이용할 수 없습니다.



변경금지. 귀하는 이 저작물을 개작, 변형 또는 가공할 수 없습니다.

- 귀하는, 이 저작물의 재이용이나 배포의 경우, 이 저작물에 적용된 이용허락조건을 명확하게 나타내어야 합니다.
- 저작권자로부터 별도의 허가를 받으면 이러한 조건들은 적용되지 않습니다.

저작권법에 따른 이용자의 권리는 위의 내용에 의하여 영향을 받지 않습니다.

이것은 [이용허락규약\(Legal Code\)](#)을 이해하기 쉽게 요약한 것입니다.

[Disclaimer](#)

의학석사 학위논문

S/G2/M synchronization observed by  
fluorescence imaging in HeLa-FUCCI  
after ionizing radiation

전리 방사선 조사 후 형광 이미징으로  
관찰한 HeLa-FUCCI의 S/G2/M  
동조화

2016 년 2 월

서울대학교 대학원  
종양생물학 협동과정  
배 성 우

A thesis of the Degree of Master of Science

**전리 방사선 조사 후 형광 이미징으로  
관찰한 HeLa-FUCCI의 S/G2/M  
동조화**

**S/G2/M synchronization observed by  
fluorescence imaging in HeLa-FUCCI  
after ionizing radiation**

**February 2016**

**Interdisciplinary Program in Cancer Biology**

**Seoul National University**

**College of Medicine**

**Seong-Woo Bae**

# ABSTRACT

**Seong-Woo Bae**

Interdisciplinary Program in Cancer Biology

The Graduate School

Seoul National University

**Objective:** Cervical cancer is the third most common cancer in women worldwide and radiotherapy is one of the major treatment methods. Radioresistance of cancer cells is a big obstacle in radiotherapy. Since the cell proliferation and therapeutic efficacy might be related to cell cycle, it is necessary to understand the radiation effects on the cell cycle.

Recently, fluorescent, ubiquitination-based cell cycle indicator (FUCCI) system was developed to visualize G1/G0 and/or S/G2/M phases of the cell cycle with distinct

colors.

In this study, I assessed the radiation effects on cell cycle using the FUCCI system.

**Methods:** Cell division of FUCCI expressing HeLa cells was observed in real time using a fluorescence microscope (Olympus IX81). G0/G1 and S/G2/M phases were determined using two different fluorescent proteins, Cdt1 and Geminin, which were activated by cell cycle specific transcription factors.

In-vitro cell studies were performed using HeLa-FUCCI cells. The cells were synchronized using 0.2 mM hydroxyurea for 24 hours, and then cells were irradiated with 6 Gy radiation using <sup>137</sup>Cs irradiator (IBL437C). The time-lapse cellular change of irradiated or non-irradiated control cells was visualized using the fluorescence microscope. FACS analysis was also performed under the

same condition.

Xenografted HeLa-FUCCI tumors were established in nude mice. One side of two tumors on each mouse in the area adjusted using multi-leaf colimators (MLC) of a linear accelerator (Clinac 6EX) was irradiated with 6 Gy. All tumors were isolated and sliced. The specimens were imaged using a fluorescence microscope combined with a TissueFAXS Plus® system. The portions of cancer cells in each cell cycle phase were calculated by the Metamorph software.

**Results:** After hydroxyurea treatment, S/G2/M phase cells measured by FACS method and fluorescence microscopy were  $62.11 \pm 3.57\%$  and  $95.91 \pm 2.00\%$ , respectively.

The S/G2/M synchronization in irradiated cells more long lasted than that in non-irradiated cells and the time

difference in the FACS and fluorescence microscopy was 4 hours and 8 hours, respectively. In the FACS data, the lowest portion of S/G2/M phase cells in non-irradiated group and irradiated group and was  $18.23 \pm 3.17\%$  at 12 hours and  $32.77 \pm 1.68\%$  at 16 hours, respectively. In the fluorescence imaging data, the lowest portion of S/G2/M phase cells in non-irradiated group and irradiated group and was  $13.05 \pm 6.84\%$  at 8 hours and  $26.39 \pm 0.12\%$  at 16 hours, respectively.

In xenograft models, the tumor at 16 hours after 6 Gy irradiation showed that the ratio of S/G2/M phase to G0/G1 phase was the highest (mAG/mKO2 =  $2.00 \pm 0.84$ ).

**Conclusion:** Radiation induced prolongation of S/G2/M synchronization in vitro cells and increase of the portion of S/G2/M phase cells in vivo mouse model. The FUCCI system can reflect radiation effects on cell cycle and

might be useful for studying the mechanism of radioresistance.

---

**Keywords:** FUCCI, ionizing radiation, cell cycle, fluorescence imaging

*Student number:* 2014-21155



# LIST OF FIGURES

<b>Figure 1. Fluorescence imaging of HeLa cells expressing the FUCCI system.....</b>	<b>16</b>
<b>Figure 2. Cytotoxicity of hydroxyurea and radiation on HeLa-FUCCI cells.....</b>	<b>19</b>
<b>Figure 3. Cell cycle synchronization of HeLa-FUCCI cells exposed to hydroxyurea.....</b>	<b>21</b>
<b>Figure 4. Radiation-induced extended cell cycle synchronization.....</b>	<b>24</b>
<b>Figure 5. Fluorescence analysis in the FUCCI expressing tumor sections following ionizing radiation.....</b>	<b>27</b>

# LIST OF ABBREVIATIONS

**FUCCI : Fluorescent, Ubiquitination-based Cell Cycle**

**Indicator**

**DSBs : DNA double-strand breaks**

**ATM : Antaxia Telangiectasia Mutated**

**NHEJ : Nonhomologous end joining**

**HRR : Homologous Recombination Repair**

**PUMA : p53 Upregulated Modulator of Apoptosis**

**HPV : Human Papillomavirus**

**FACS : Fluorescence Activated Cell Sorting**

**DMEM : Dulbecco' s Modified Eagle' s Medium**

**FBS : Fetal Bovine Serum**

**PBS : Phosphate-buffered saline**

# CONTENTS

<b>Abstract.....</b>	<b>i</b>
<b>Contents.....</b>	<b>viii</b>
<b>List of figures.....</b>	<b>vi</b>
<b>List of abbreviations.....</b>	<b>vii</b>
<b>Introduction.....</b>	<b>1</b>
<b>Material and Methods.....</b>	<b>6</b>
<b>Results.....</b>	<b>12</b>
<b>Discussion.....</b>	<b>30</b>
<b>References.....</b>	<b>33</b>
<b>Abstract in Korean.....</b>	<b>40</b>

# INTRODUCTION

## I. The necessity of studying the radiation effects on cell cycle

Cervical cancer is the third most common cancer worldwide among gynecologic cancers [1]. Although radiotherapy have been used in this cancer, radioresistance is a big problem [2].

Ionizing radiation can cause DNA double-strand breaks (DSBs) [3]. The DNA damage activates antaxia telangiectasia mutated (ATM) and then ATM phosphorylates p53 tumor suppressor protein [4]. The phosphorylated p53 protein plays an important role in cell cycle control and apoptosis.

In mammalian cells, two cell cycle checkpoints are mediated for the repair of DSBs after exposure to the radiation: one at the G1/S transition and the other at

G2/M transition. During the checkpoints, the repair process occurs through one of two repair mechanisms: nonhomologous end joining (NHEJ) and homologous recombination repair (HRR). In NHEJ, DNA ligase IV utilizes overhanging pieces of DNA neighbouring to the break to join and fill in the ends. In HRR, the homologous chromosome itself is used as a template for repair [3].

If the damage exceeds, the phosphorylated p53 activates genes that produce proteins involved in apoptosis. p53 upregulated modulator of apoptosis (PUMA), one of the proteins, promotes apoptosis by binding to and inactivating the Bcl2 protein, an anti-apoptotic protein [5].

In p53-defective cancer cells, however, it is possible to grow in an unlimited fashion avoiding apoptosis. The lack of functional p53 tumor suppressor gene allows accumulation of Bcl2 protein and results in radioresistance

blocking apoptosis [6].

Therefore, it is necessary to investigate the radiation effects on cell cycle in p53-defective cancer cells.

## **II. FUCCI as a system to visualize cell cycle**

There are many methodologies for cell cycle study such as monitoring morphological changes in dividing cells, FACS analysis of DNA content stained with either propidium iodide (PI) or 4',6'-diamidino-2-phenylindole (DAPI) and detection of 5'-bromo-2'-deoxyuridine (BrdU) labeled to the DNA-replicating cells [7-9]. However, there were no methods which can visualize the alteration of cell cycle in living cells in real time.

Recently, fluorescent, ubiquitination-based cell cycle indicator (FUCCI) developed by Sakaue-Sawano et al. [7] has been used for visualizing cell cycle phases. The

principle of this system is the use of inversely oscillating level of Cdt1 and Geminin proteins.

Cdt1 protein is a DNA replication licensing factor expressed in G1 phase. The expression of Cdt1 is regulated by cell cycle-specific ubiquitination mediated by an E3 ligase, SCF<sup>Skp2</sup>. Geminin protein which is a Cdt1 inhibitor is also regulated by cell cycle-specific ubiquitination, in this case, mediated by APC<sup>Cdh1</sup>. Geminin expression is observed in S/G2/M phases [10].

These proteins were fused to monomeric Kusabira Orange 2 (mKO2) and monomeric Azami Green (mAG), respectively. Consequently, by introducing the FUCCI, the G0/G1 and S/G2/M phases can be visualized in red fluorescence and green fluorescence, respectively (Figure 1a).

The FUCCI system has been widely used for cell cycle research in many studies [11-17]. Although the

FUCCI has some disadvantages that it cannot reflect S/G2 transition and recognize cell types and differentiation states based on cell morphologies [18], it has great advantages such as visualization of cell cycle phase in living cells and analyzing cell cycle in locally distributed population within tumors [19].

### **III. Purpose of this study**

Although radiation effects on cell cycle have been reported in many studies, radioresistance still remains unclear [17]. It is important to understand radiation effects on cell cycle in HeLa cells known to be infected by human papilloma virus (HPV) which induces p53 degradation and deficiency [20] for improving therapeutic strategies.

In the present study, I evaluated the effects of radiation on cell cycle in HeLa cells, using FUCCI system was used both in vitro and in vivo.



# **MATERIALS AND METHODS**

## **Cell culture**

HeLa-FUCCI cells (RCB2812) were purchased from RIKEN Bio Resource Center, Japan. Cells were grown in Dulbecco's Modified Eagle's Medium (DMEM, Welgene, Daegu, Korea) containing 10% (v/v) fetal bovine serum (FBS, Invitrogen, Grand Island, NY, USA) and 1% Antibiotic-Antimycotic (Gibco BRL, Grand Island, NY, USA).

## **Cytotoxicity test of hydroxyurea**

To determine toxicity of hydroxyurea, a ribonucleotide reductase inhibitor, which is used for S-phase synchronization, cell counting kit-8 (CCK-8) was performed according to the manufacturer's protocol.

Briefly, 5,000 cells/well were seeded in a 96-well plate. Hydroxyurea (Sigma, St. Louis, MO, USA) in the range of 0.2 mM to 1 mM was added to each well and incubated for 17 hours. Cell viability was measured by reading the optical density at 450 nm after adding WST-8 [2-(2-methoxy-4-nitrophenyl)-3-(4-nitrophenyl)-5-(2,4-disulfophenyl)-2H-tetrazolium, monosodium salt; Dojindo] mixture and incubation for 2 hours.

## **Ionizing irradiation**

HeLa-Fucci cells were irradiated at a dose of 6 Gy in a IBL 437C blood irradiator. One side of two established tumors on each BALB/c nude mouse in range of the field generated using MLCs of a Clinac 6EX linear accelerator (Varian, Palo Alto, CA, USA) was irradiated with 6 Gy (Figure 5a).

## **Clonogenic assay**

HeLa-FUCCI cells were seeded at a density 400 of cells per well in six-well culture dishes and irradiated with various doses (0, 1, 2, 3, 4, 5, and 6 Gy). After incubation for 10 days, the colonies in each well was stained with crystal violet to calculate cell viability *in vitro*.

## **Flow Cytometry Analysis**

Trypsinized cells and collected supernatant were centrifuged together. Cells were fixed in 70% ethanol in Phosphate-buffered saline (PBS) for few days. The fixed cells were washed in PBS and incubated in 0.5  $\mu\text{g}/\mu\text{l}$  Rnase A (Bio Basic, Canada) for at least 30 minutes in 37°C water bath. After adding 20  $\mu\text{l}$  of 7-AAD Staining Solution (BD Bioscience), the cells were incubated for 1

hour at room temperature. Samples were analyzed using a FACS Canto II flow cytometer (BD Bioscience).

## **Fluorescence imaging of HeLa-FUCCI cells**

To check the fluorescence expressions in each phase, confocal laser microscopy was performed. Briefly, 5,000 cells (HeLa-FUCCI cells) were seeded in a 35mm confocal dish and taken by a confocal laser microscope (Leica TCS SP8, Germany). For time-lapese imaging, 5,000 cells (HeLa-FUCCI cells) were seeded in each well of a 8-well glass bottom chamber and irradiated with 6 Gy after treatment of 0.2 mM hydroxyurea for 24 hours. All fluorescence images were taken for 16 hours using a fluorescence microscope (Olympus IX81, Troy, NY, USA). By counting the fluorescence emitted from nuclei in the

cells, the fluorescence images were analyzed.

## **Xenograft modeling**

Four-week-old female BALB/c nude mice were purchased from the Orient Bio Inc., (Seongnam, Korea). HeLa-FUCCI cells ( $2 \times 10^6$ ) were suspended in 20  $\mu$ l culture media and 80  $\mu$ l matrigel and then injected subcutaneously into each flank of BALB/c nude mice.

## **Fluorescence imaging of tumor sections**

FUCCI-expressing HeLa xenograft tumors were extracted and were fixed for 24 hours in 4% paraformaldehyde in PBS. After paraffin embedding, the specimens were cut into 4  $\mu$ m sections. The slides were incubated in a 67 °C oven for 1 hour to melt the paraffin and mounted with ProLong® Gold antifade reagent

(Invitrogen, Grand Island, NY, USA). Using a Zeiss AxioImager Z1 fluorescence microscope system with an automated acquisition system TissueFAXS Plus® (TissueGnostics, Vienna, Austria), fluorescence images for each slide were acquired. The fluorescence intensity for the whole tumor area was analyzed with the MetaMorph Image Analysis Software (Molecular Devices, LLC, Sunnyvale, CA, USA).

## **Statistical analysis**

Results were presented as the mean of percentage standard error. The Mann-Whitney U test was conducted to measure P value. P values < 0.05 were considered to be statistically significant.

## RESULTS

### **Classification of cell cycle phases in cells expressing the FUCCI probes**

A typical fluorescence image of FUCCI expressing HeLa cells shows distinct colors that red, yellow and green represent G<sub>1</sub>-, early S- and S/G<sub>2</sub>/M-phase cells respectively were observed during the culture period. (Figure 1b). To confirm whether the colors indicate G<sub>0</sub>/G<sub>1</sub> and S/G<sub>2</sub>/M phases determined by Cdt1 and Geminin, respectively, a single cell was monitored using a fluorescence microscope. The cell cycle began with a green color and as the cycle continued the cell changed colors and then turned back to the green color (Figure 1c). This means that the FUCCI system in proliferating cells was working appropriately.

## **Optimal condition of hydroxyurea and ionizing radiation to induce cytotoxicity of cancer cells**

For kinetic analyses of cell cycle progression, it was needed to develop the experimental condition that allows synchronization in S phase of the first cycle. Before using hydroxyurea to synchronize cell cycle, the non-toxic concentration was decided in 0.2 mM through cytotoxicity test (Figure 2a). The most lethal radiation dose was decided in 6 Gy ( $0.0056 \pm 0.0066\%$  cells survived) through the clonogenic survival assay (Figure 2b).

### **Analysis of hydroxyurea-induced cell cycle synchronization**

After 0.2 mM hydroxyurea treatment, the cell cycle was analyzed by comparison between FACS analysis and fluorescence imaging. In the FACS analysis, S/G2/M



cells increased from  $38.60 \pm 1.37\%$  to  $62.11 \pm 3.57\%$  (Figure 3a). In the fluorescence images, S/G2/M cells increased from  $56.66 \pm 10.78\%$  to  $95.91 \pm 2.00\%$  (Figure 3b).

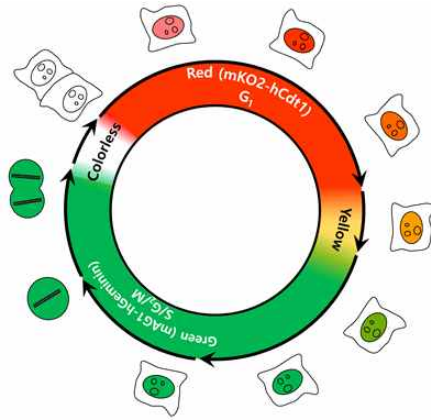
## **Radiation effects on cell cycle synchronization**

According to the FACS data, the portion of S/G2/M phase cells in the non-irradiated group was the lowest at 12 hours ( $18.23 \pm 3.17\%$ ). The portion of S/G2/M phase cells in the irradiated group was the lowest at 16 hours ( $32.77 \pm 1.68\%$ ) (Figure 4a). According to the time-lapse imaging, the portion of S/G2/M phase cells in the non-irradiated group was the lowest at 8 hours ( $13.05 \pm 6.84\%$ ). The portion of S/G2/M phase cells in the irradiated group was the lowest at 16 hours ( $26.39 \pm 0.12\%$ ) (Figure 4b). These results showed that radiation induced cell cycle arrest in S/G2/M phase.

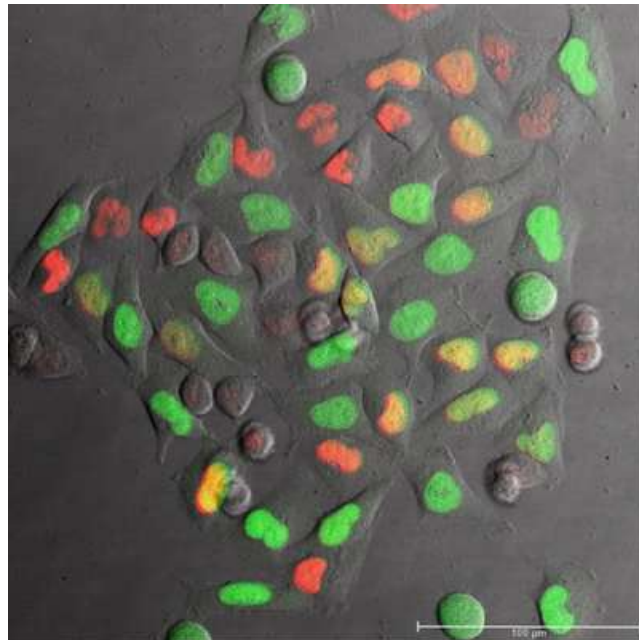
## Visualizing the fluorescence distributions in HeLa-FUCCI tumors

Fluorescence images indicated that S/G2/M phase at 16 hours post-irradiation was abundant unlike non-irradiated control group and irradiated group at 24 hours (Figure 5a). In the non-irradiated group, the mAG/mKO2 ratio obtained from the fluorescence calculated using the MetaMorph software showed  $0.98 \pm 0.10$  and  $1.35 \pm 0.19$  at 16 hours and 24 hours, respectively. In the irradiated group, the ratio was  $2.00 \pm 0.84$  and  $1.20 \pm 0.63$  at 16 hours and 24 hours, respectively. This result indicated that radiation induced S/G2/M arrest in the tumor at 16 hours.

(a)



(b)



(c)

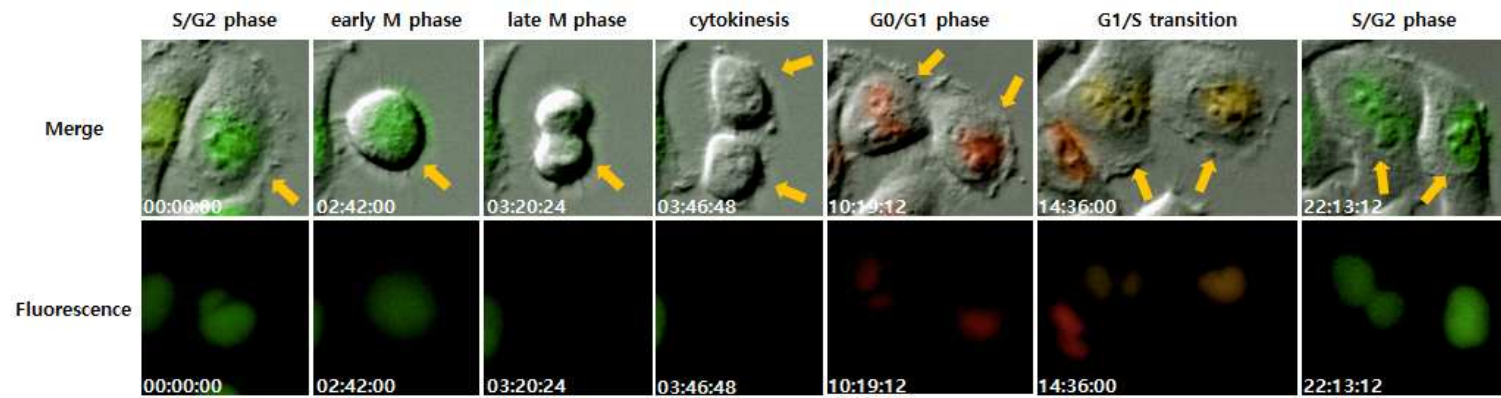


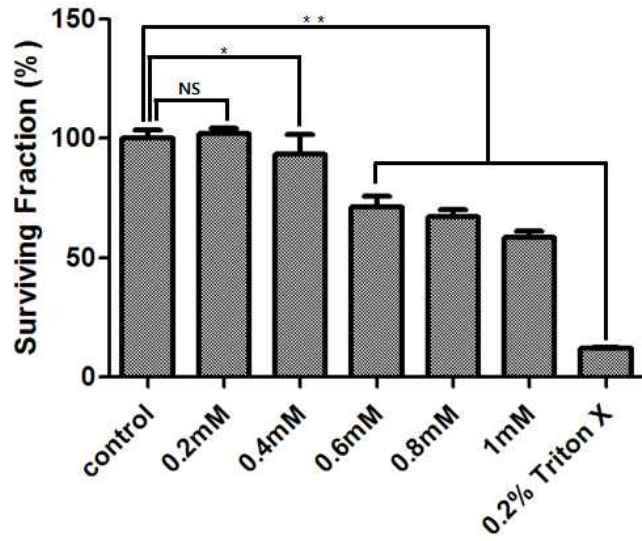
## **Figure 1. Fluorescence imaging of HeLa cells expressing the FUCCI system**

(a) Schematic overview of the FUCCI system. The system had three colors. Red, yellow, and green indicate G0/G1 phase, G1/S transition, and S/G2/M phase, respectively.

(b) A representative confocal microscopy image of HeLa-FUCCI cells representing cytokinesis/early G1 (no fluorescence), G0/G1 (red), G1/S transition (yellow), and S/G2/M (green). Scale bar represents 100  $\mu\text{m}$ .

(c) Time-lapse images of HeLa-FUCCI cells. Cell division of a single cell can be monitored (yellow arrow).

(a)



(b)

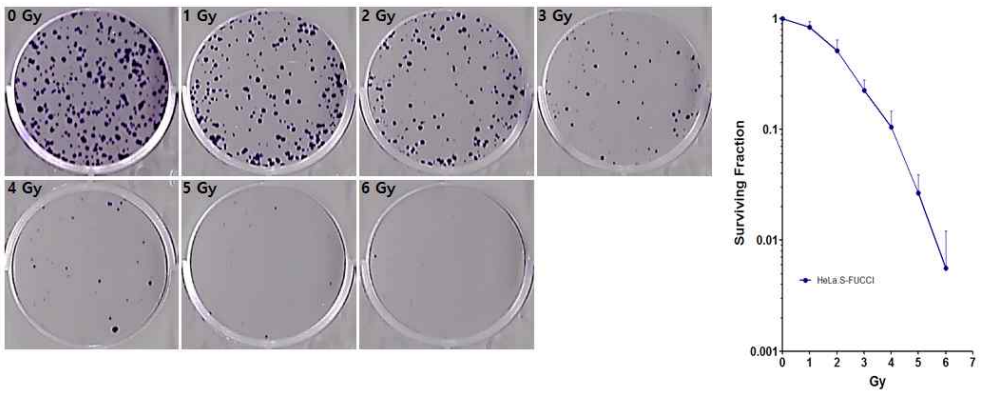
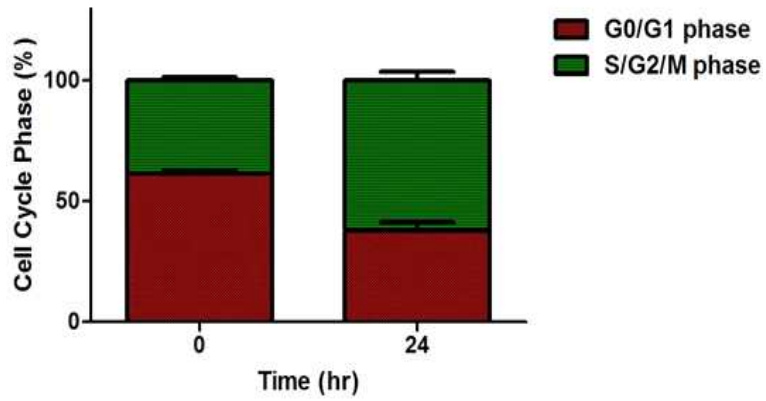
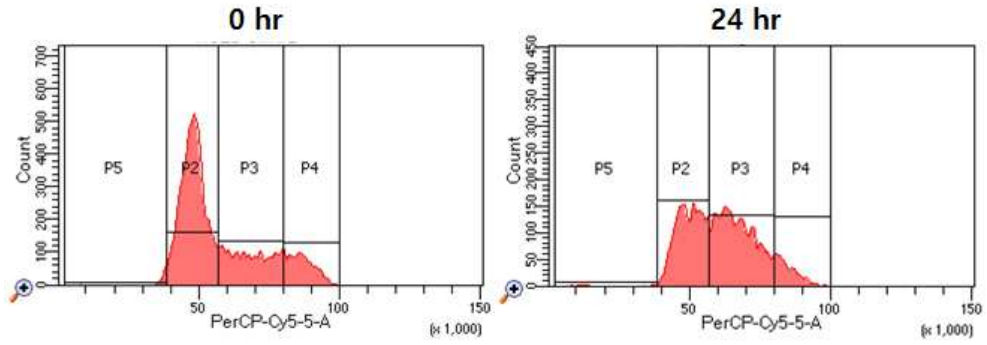


## **Figure 2. Cytotoxicity of hydroxyurea and radiation on HeLa-FUCCI cells**

(a) Cytotoxicity of hydroxyurea was measured using a Cell Counting Kit-8 (CCK-8) indicates that 0.2 mM is non-toxic. NS, non-significant difference, \*,  $p < 0.05$ , \*\*,  $p < 0.001$ .

(b) The cell survival curve derived from clonogenic assay for HeLa-FUCCI. The surviving fraction (SF) of irradiated cells was normalized to the plating efficiency (PE) of non-irradiated controls. Data show the average SF  $\pm$  standard deviation (SD).

(a)





(b)

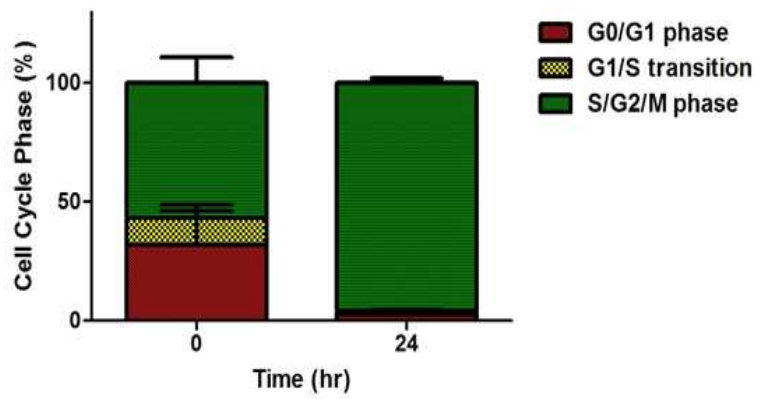
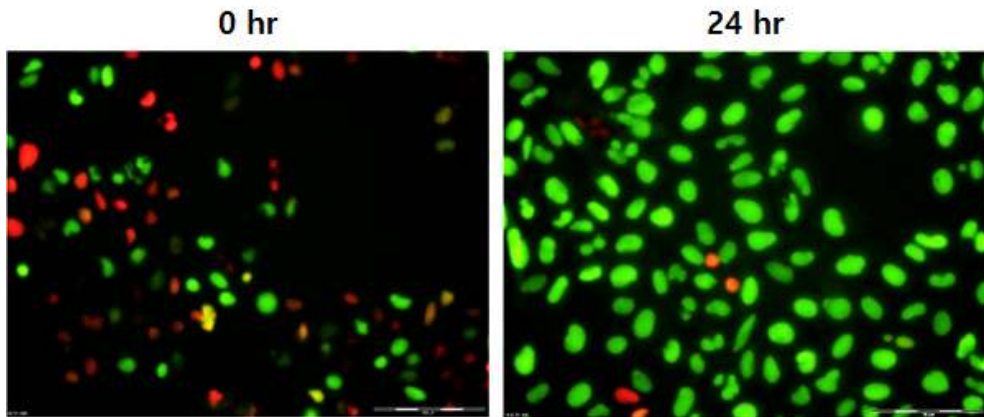
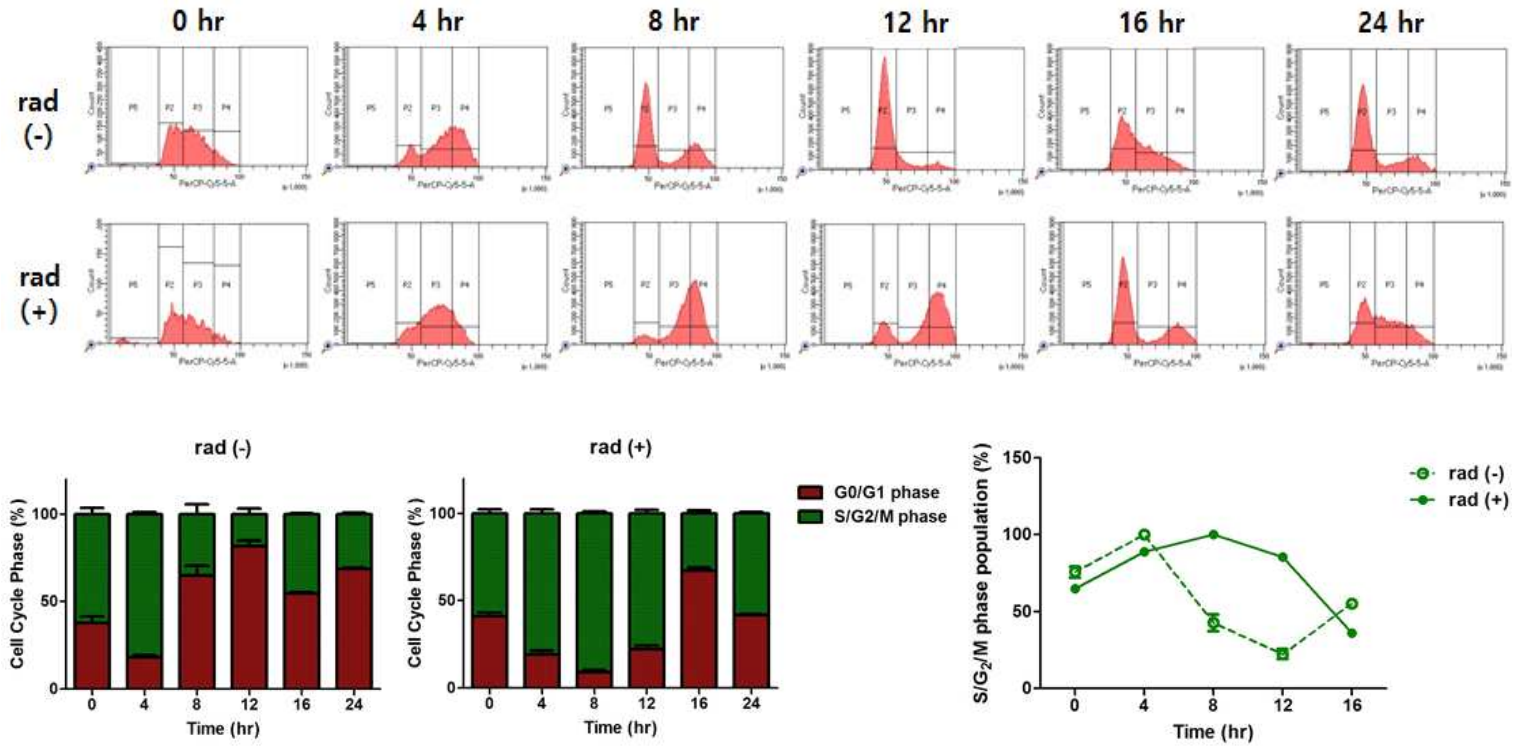


**Figure 3. Cell cycle synchronization of HeLa-FUCCI cells exposed to hydroxyurea**

(a) FACS analysis of HeLa-FUCCI cells after hydroxyurea treatment. The histogram represents the portion of G0/G1 phase and S/G2/M phase.

(b) Fluorescence imaging of HeLa-FUCCI cells after hydroxyurea treatment. The histogram represents the portion of G0/G1 phase, G1/S transition and S/G2/M phase.

(a)



(b)

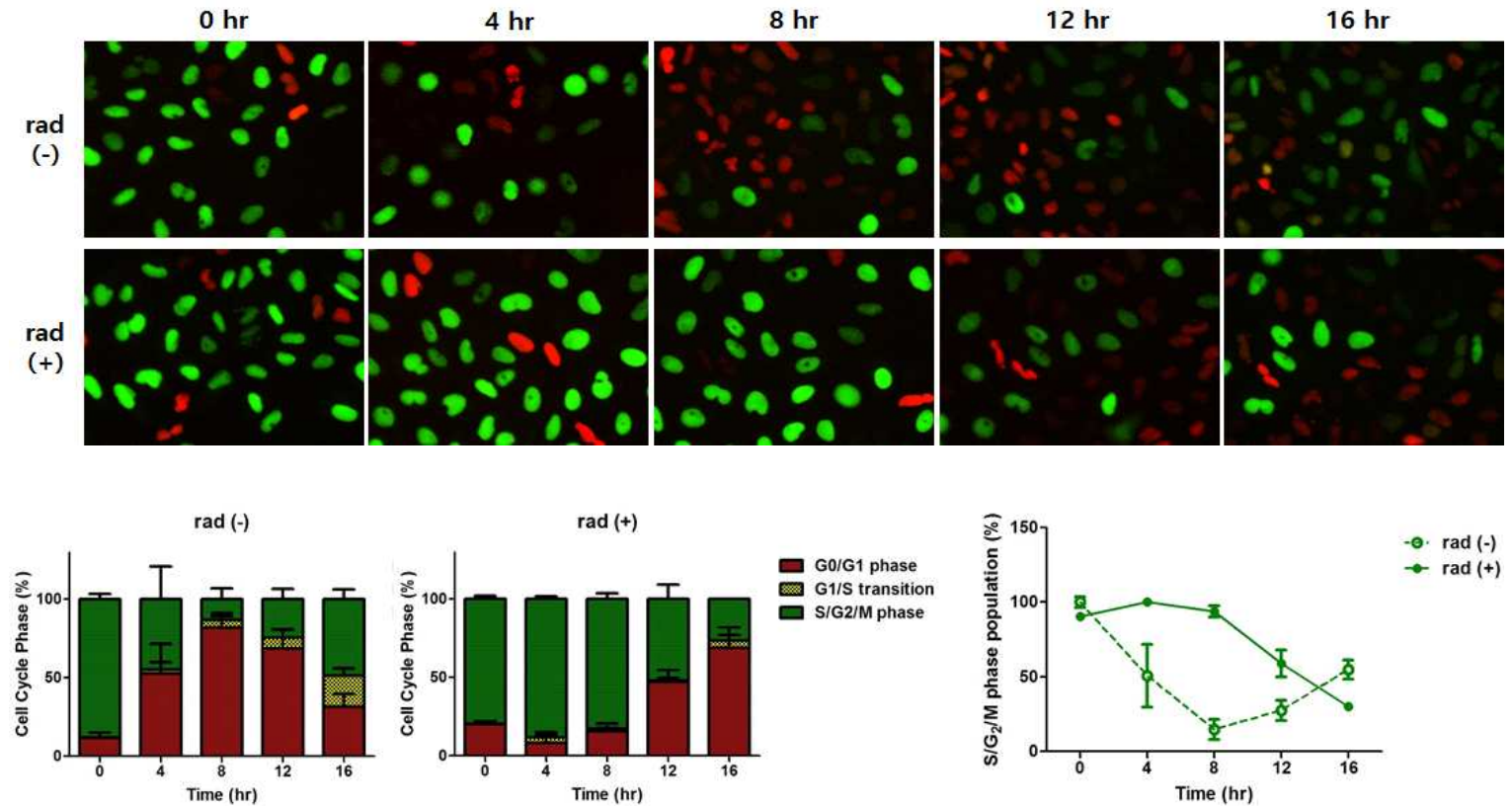
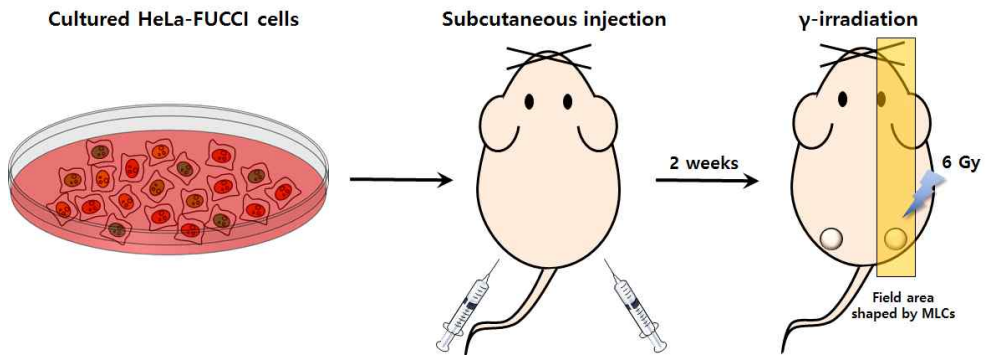


## **Figure 4. Radiation-induced extended cell cycle synchronization**

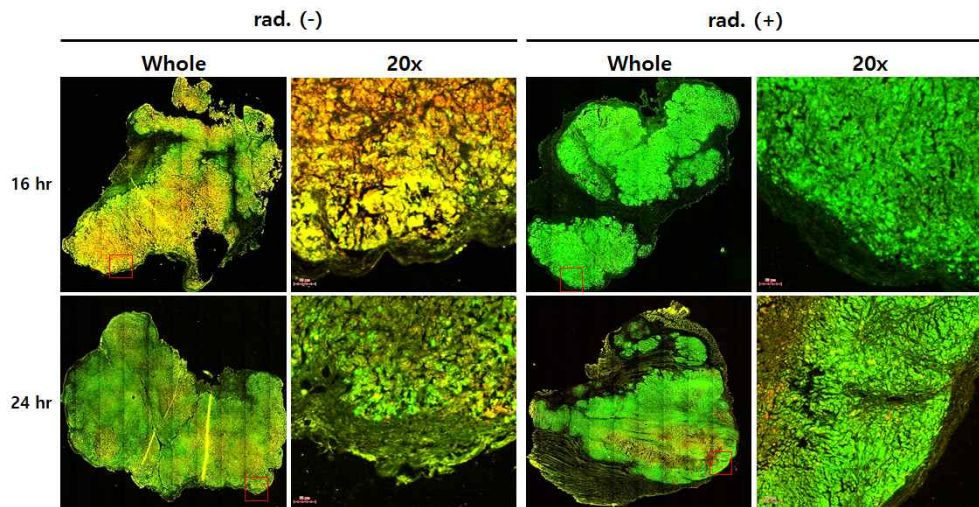
(a) FACS analysis of the synchronized cells after irradiation. The curves for the time difference indicate change of the portion of S/G2/M phase cells.

(b) Time-lapse images of the synchronized cells after irradiation. The curves for the time difference indicate change of the portion of S/G2/M phase cells.

(a)



(b)



(c)

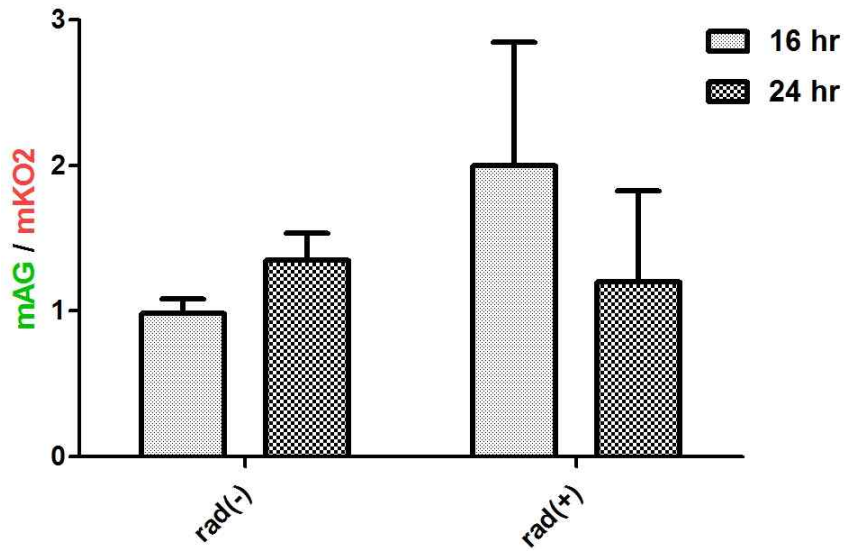


**Figure 5. Fluorescence analysis in the FUCCI expressing tumor sections following ionizing radiation**

(a) Schematic of the experiment. After the xenopplantation, one side of two generated tumors in the field area (yellow box) adjusted using MLCs of a linear accelerator was irradiated.

(b) Representative fluorescence images of tumor sections at the indicated times. Scale bar represents 50  $\mu\text{m}$ .

(c) Calculation of the fluorescence intensity using the MetaMorph Software.



## DISCUSSION

In this study, I found that S/G2/M synchronization of HeLa-FUCCI cells was increased following ionizing radiation both in-vitro cell study and in-vivo mouse model. These results show that ionizing radiation may induce G2/M arrest in HeLa cells, as reported [21]. It is considered that the G2/M arrest is related with the resistance to ionizing radiation in HeLa cells.

It has been shown that subpopulation within a tumor is heterogeneous [22]. In many cancers, glucose and oxygen supply are highly required. Moreover, cancers newly build circulatory system as they outgrow the capillary system of normal tissues. The newly built system tends to have inefficient and asymmetric vascular function. Assymmetric nutrient deprivation in different areas in the tumor is regarded as a main driver of the tumor

heterogeneity. A part of the nutrient deprived cells such as hypoxic cells might develop radioresistance while subpopulations might also undergo necrosis.

Under hypoxic condition, hypoxia-inducible factor 1  $\alpha$  (HIF1  $\alpha$ ) is stabilized. Radiotherapy also contributes to the stabilization by causing tumor reoxygenation, an increase in levels of reactive oxygen species (ROS) [23]. Hypoxia promotes vascular endothelial growth factor A (VEGFA) production, leading to the formation of abnormal vessels. The vasculogenesis aids tumor recurrence after radiotherapy.

Although many studies have dealt with radioresistant cancer, the mechanisms with respect to cell cycle in radioresistant cancer cells are still poorly understood [17]. For instance, mammalian cells generally have features of radiosensitivity depending on cell cycle

phase: the most radioresistant S phase and the most radiosensitive M phase. However, the precise molecular mechanism of these phenomena has not been fully elucidated.

In the present study, I visualized radiation effects on cell cycle using the FUCCI system. I propose that the FUCCI might be useful for mechanism study of radioresistance in heterogeneous cancer cells.

## REFERENCES

- [1] Siegel R, Ward E, Brawley O, Jemal A. Cancer statistics, 2011: the impact of eliminating socioeconomic and racial disparities on premature cancer deaths. *CA Cancer J Clin.* 61:212-36 (2011).
- [2] Kim TJ, Lee JW, Song SY, Choi JJ, Choi CH, Kim BG, Lee JH, Bae DS. Increased expression of pAKT is associated with radiation resistance in cervical cancer. *Br J Cancer.* 94:1678-82 (2006).
- [3] Dana Branzei, Marco Foiani. Regulation of DNA repair throughout the cell cycle. *Nat Rev Mol Cell Biol.* 9(4):297-308 (2008).
- [4] Valerie K, Povirk LF. Regulation and mechanisms of mammalian double-strand break repair. *Oncogene.* 22(37):5792-812 (2003).

- [5] Nakano K, Vousden KH. PUMA, a Novel Proapoptotic Gene, Is Induced by p53. *Mol Cell*. 7(3):683-94 (2001).
- [6] Lee JM, Bernstein A. p53 mutations increase resistance to ionizing radiation. *Proc Natl Acad Sci U S A*. 90(12):5742-6 (1993).
- [7] Sakaue-Sawano A, Kurokawa H, Morimura T, Hanyu A, Hama H, Osawa H, Kashiwagi S, Fukami K, Miyata T, Miyoshi H, Imamura T, Ogawa M, Masai H, Miyawaki A. Visualizing spatiotemporal dynamics of multicellular cell-cycle progression. *Cell*. 132:487 - 98 (2008).
- [8] Darzynkiewicz Z. Critical aspects in analysis of cellular DNA content. *Curr Protoc Cytom*. Chapter 7:Unit 7.2. (2011).
- [9] Poot M, Silber JR, Rabinovitch PS. A novel flow cytometric technique for drug cytotoxicity gives results comparable to colony-forming assays. *Cytometry*. 48(1):1-5

(2002).

[10] Nishitani, H., Lygerou, Z., Nishimoto, T. Proteolysis of DNA replication licensing factor Cdt1 in S-phase is performed independently of geminin through its N-terminal region. *J. Biol. Chem.* 279:30807-16 (2004).

[11] Honda-Uezono A, Kaida A, Michi Y, Harada K, Hayashi Y, Hayashi Y, Miura M. Unusual expression of red fluorescence at M phase induced by anti-microtubule agents in HeLa cells expressing the fluorescent ubiquitination-based cell cycle indicator (Fucci). *Biochem Biophys Res Commun.* 428(2):224-9 (2012).

[12] Nahar K, Goto T, Kaida A, Deguchi S, Miura M. Effects of Chk1 inhibition on the temporal duration of radiation-induced G2 arrest in HeLa cells. *J Radiat Res.* 55(5):1021-7 (2014).

[13] Malka Y, Eden S. Analysis of apoptosis in FUCCI

HeLa cells. *Cytometry A*. 79(4):243-6 (2011).

[14] Miwa S, Yano S, Tome Y, Sugimoto N, Hiroshima Y, Uehara F, Mii S, Kimura H, Hayashi K, Efimova EV, Fujiwara T, Tsuchiya H, Hoffman RM. Dynamic color-coded fluorescence imaging of the cell-cycle phase, mitosis, and apoptosis demonstrates how caffeine modulates cisplatin efficacy. *J Cell Biochem*. 114(11):2454-60 (2013).

[15] Yano S, Tazawa H, Hashimoto Y, Shirakawa Y, Kuroda S, Nishizaki M, Kishimoto H, Uno F, Nagasaka T, Urata Y, Kagawa S, Hoffman RM, Fujiwara T. A genetically engineered oncolytic adenovirus decoys and lethally traps quiescent cancer stem-like cells in S/G2/M phases. *Clin Cancer Res*. 19(23):6495-505 (2013).

[16] Yano S, Miwa S, Mii S, Hiroshima Y, Uehara F, Kishimoto H, Tazawa H, Zhao M, Bouvet M, Fujiwara T,

Hoffman RM. Cancer cells mimic in vivo spatial-temporal cell-cycle phase distribution and chemosensitivity in 3-dimensional Gelfoam® histoculture but not 2-dimensional culture as visualized with real-time FUCCI imaging. *Cell Cycle*. 14(6):808-19 (2015).

[17] Nakayama M, Kaida A, Deguchi S, Sakaguchi K, Miura M. Radiosensitivity of early and late M-phase HeLa cells isolated by a combination of fluorescent ubiquitination-based cell cycle indicator (Fucci) and mitotic shake-off. *Radiat Res*. 176(3):407-11 (2011).

[18] Zielke N, Edgar BA. FUCCI sensors: powerful new tools for analysis of cell proliferation. *Wiley Interdiscip Rev Dev Biol*. 4(5):469-87 (2015).

[19] Yano S, Miwa S, Mii S, Hiroshima Y, Uehara F, Yamamoto M, Kishimoto H, Tazawa H, Bouvet M, Fujiwara T, Hoffman RM. Invading cancer cells are predominantly in



G0/G1 resulting in chemoresistance demonstrated by real-time FUCCI imaging. *Cell Cycle*. 13(6):953-60 (2014).

[20] Eileen M. Burd. Human Papillomavirus and Cervical Cancer. *Clin Microbiol Rev*. 16(1): 1-17 (2003).

[21] Tamamoto T, Ohnishi K, Takahashi A, Wang X, Yosimura H, Ohishi H, Uchida H, Ohnishi T. Correlation between gamma-ray-induced G2 arrest and radioresistance in two human cancer cells. *Int J Radiat Oncol Biol Phys*. 1;44(4):905-9 (1999).

[22] Stuart K. Calderwood. Tumor Heterogeneity, Clonal Evolution, and Therapy Resistance: An Opportunity for Multitargeting Therapy. *Discov Med*. 15(82): 188-94 (2013).

[23] Barker HE, Paget JT, Khan AA, Harrington KJ. The tumour microenvironment after radiotherapy: mechanisms of resistance and recurrence. *Nat Rev Cancer*.

15(7):409-25 (2015).

## 국문초록

**목적:** 자궁경부암은 세계에서 여성 암 중 세 번째로 빈번한 암이고 방사선치료가 주요 치료법이다. 암세포의 방사선 저항성은 방사선치료에서 큰 장애물이다. 세포 증식과 치료 효과는 세포주기와 관련이 있으므로 세포주기의 방사선 효과를 이해하는 것은 중요하다. 최근에 개발된 세포주기 형광 프로브 (FUCCI)는 G0/G1기와 S/G2/M기를 구분되는 색깔로 볼 수 있는 시스템이다. 이 논문에서는 FUCCI 시스템을 이용하여 방사선이 세포분열에 미치는 영향을 평가하였다.

**방법:** FUCCI를 발현하는 HeLa의 세포분열을 형광 현미경 (Olympus IX81)을 사용하여 실시간으로 관찰하였다. G0/G1기와 S/G2/M기를 세포 주기에 특이적인 전사인자에 의해 활성화된 두 형광 단백질인 Cdt1과 Geminin을 이용하여 결정하였다. HeLa-FUCCI 세포에 0.2 mM 하이드록시유리아를 24시간동안 처리하여 세포주기를 동조화하였고, <sup>137</sup>Cs 조사기 (IBL437C)로 6 Gy 방사선을 조사하였다. 방사선이 조사된 세포와 조사되지 않은 대조군의 시간적 변화를 형

광 현미경으로 촬영하였다. 동일조건 하에 FACS 분석을 하였다. 누드 마우스에 이중 이식 HeLa-FUCCI 종양을 구축하였다. 각각의 마우스 내 두 종양 중 선형 가속기 (Clinac 6EX)의 다엽콜리메이터 (MLC)에 의해 조절된 영역에 있는 한 쪽에만 6 Gy 방사선을 조사하였다. 모든 종양을 적출하여 절편하였다. 표본은 티슈팩스 시스템이 결합된 형광 현미경 (Zeiss Axioimager Z1)으로 촬영하였다. 메타모프 소프트웨어를 이용하여 각각의 세포주기에 해당하는 암세포의 분포를 계산하였다.

**결과:** 하이드록시유리아를 처리 후 S/G2/M기 세포는 FACS에서  $62.11 \pm 3.57\%$  그리고 형광 현미경 관찰에서  $95.91 \pm 2.00\%$ 였다. S/G2/M기 동조화는 방사선이 조사된 세포에서 대조군의 세포보다 오래 지속되었고, 그 시간 차는 FACS에서 4시간, 그리고 형광 현미경에서 8시간이었다. FACS 데이터의 경우, S/G2/M기 세포가 가장 낮았을 때는 대조군에서 12시간일 때 ( $18.23 \pm 3.17\%$ )였고, 방사선이 조사된 군에서 16시간일 때 ( $32.77 \pm 1.68\%$ )였다. 형광 이미징 데이터의 경우, S/G2/M기 세포가 가장 낮았을 때는 대조군에서 8시간일 때

( $13.05 \pm 6.84\%$ )였고, 방사선이 조사된 군에서 16시간일 때 ( $26.39 \pm 0.12\%$ )였다. 이중 이식 모델의 경우, 6 Gy를 조사 후 16시간째 종양에서 S/G2/M기 대 G0/G1기의 비율이 가장 높았다 ( $mAG/mKO2 = 2.00 \pm 0.84$ ).

**결론:** 방사선의 영향으로 세포 수준에서 S/G2/M 동조화가 늘어났고, 마우스 모델에서 S/G2/M기 세포의 분포가 증가했다. FUCCI 시스템은 방사선이 세포주기에 미치는 영향을 반영할 수 있으며, 암에서 방사선저항성 기전을 연구하는데 유용할 수 있다.

---

**핵심어:** FUCCI, 전리 방사선, 세포 주기, 형광 이미징

**학번:** 2014-21155